

Ethanol sensing properties of porous ZnO spheres via hydrothermal route

Wenchuang Wang · Yongtao Tian ·
Xinchang Wang · Hao He · Yurui Xu ·
Chuan He · Xinjian Li

Received: 9 October 2012 / Accepted: 17 December 2012 / Published online: 8 January 2013
© Springer Science+Business Media New York 2013

Abstract ZnO spheres composed of porous flakes were prepared by template-free, economical hydrothermal method combined with heat treatment. The high-density pores with the size in tens of nanometers were found distributed through each piece of the flake. The sensor based on porous ZnO spheres showed improved ethanol response compared to that based on commercial ZnO powders. ZnO spheres sensor showed obvious response to 2 ppm ethanol at the operation temperature of 280 °C, with the corresponding response value of 2.8 and the response and recovery times of 10 and 15 s, respectively. The response of the sensor increased linearly with the concentration of ethanol in the range of 2–500 ppm. The good sensing performance of the ZnO sphere sensor to ethanol gas indicated that the ZnO sphere could be a promising candidate as the building block for highly sensitive and reliable gas sensor.

Introduction

Gas sensors have been intensively studied due to their widely and important applications in environment monitoring, medical detection, food industry, mining industry,

bio-engineering, and defense safety [1–6]. Ever since Seiyama et al. [7] discovered that the electrical conductivity of ZnO could be dramatically changed by the presence of reactive gases in air in 1962, metal-oxide semiconductors have received considerable attention among lots of gas-sensing materials because of their high sensitivity, fast response, quick recovery, excellent stability, and ease in preparation [8–10]. ZnO, as one of the most attractive materials, has been extensively developed. It is known that unintentionally doped ZnO always display n-type behavior and the responsible donors are usually identified as the O vacancy (V_O), the Zn interstitial (Zn_I), or the defect complex [11–13]. Thus, when a ZnO gas sensor is exposed to reducing ambient, the reducing molecules will react with oxygen ions on the sensor surface and the electrons released from the surface reaction will transfer back into the conduction band, resulting in the increase of the conductivity.

In recent years, gas sensors based on various nanostructure materials have been reported, such as nanowires [4], nanorods [9], nanotubes [5], hollow spheres [10], and porous nanosheets [1]. Among them, porous materials have been brought to attentions of more researchers. Liu et al. [1] prepared porous ZnO nanosheets using ethanediamine for indoor air containment detection. Hyodo et al. [14] synthesized macroporous SnO_2 film using PMMA for NO_x detection. Zhang et al. [15] fabricated SnO_2 hollow sphere gas sensor using carbonaceous polysaccharide microspheres as template. Sensors based on the porous structures could contribute to improve sensing performances because of the large active surface area and efficient gas diffusion induced by this unique structure. The conventional methods for preparing porous or hollow materials usually require the use of pore-directing reagents or templates and may suffer from contamination [1, 14, 15]. Thus, a facile,

W. Wang · Y. Tian (✉) · X. Wang · H. He · Y. Xu · C. He ·
X. Li

Department of Physics and Laboratory of Material Physics,
Zhengzhou University, Zhengzhou 450052, People's Republic of
China
e-mail: tianytao@sina.com

W. Wang
e-mail: wenchuangwang@163.com

Y. Tian
Henan Ancai High-technology Co., Ltd, Henan 455000, Anyang,
People's Republic of China

economical, template-free method for producing porous materials is of great significance.

Herein, we synthesized ZnO spheres composed of porous flakes via a template-free, economical hydrothermal route combined with heat treatment. ZnO spheres were used as sensing material for the gas detection. The temperature-dependent and concentration-dependent sensing behaviors of the ZnO spheres to ethanol were studied. The obtained results show that ZnO spheres would be promising material for preparing the sensors with good gas-sensing properties.

Experimental section

Materials and synthesis

The fabrication strategy was initiated by Hosono et al. [16], who first fabricated layered hydroxide zinc salt (LHZS) films as self-template precursors. The porous ZnO structures were obtained after heat treatment. However, in our study, no organic solvent or surfactant was used.

In a typical procedure, 4 mmol zinc nitrate (Beijing Huateng Chemical Co., Ltd.) and 8 mmol urea (Shantou Xilong Chemical Co., Ltd.) were dissolved in 40 ml aqueous solution under stirring (All chemicals were analytical pure grade and used without further purification), and have been used all the time. Then, the mixture was transferred into 50 ml Teflon-lined autoclave and maintained at 120 °C for 2 h. The resulting product was isolated by centrifugation, cleaned by three cycles of centrifugation/washing/redispersion in water and ethanol alternately, and then dried at 60 °C for 12 h. Finally, the product was annealed in air at 450 °C for 2 h with a heating rate of 5 °C/min.

Characterization

The phase characterization of the products was done by X-ray powder diffractometer (XRD, Philips X) with Cu K α as the radiation source and operated at 40 kV and 30 mA.

The morphology was characterized using a field emission scanning electron microscope (FE-SEM, JEOL F6700) and transmission electron microscopy (TEM, JOEL JEM2100). The Brunauer–Emmett–Teller (BET) surface area and BJH pore size distribution of the powders were analyzed by nitrogen physisorption at 77 K on a Quantachrome NOVA 1000e.

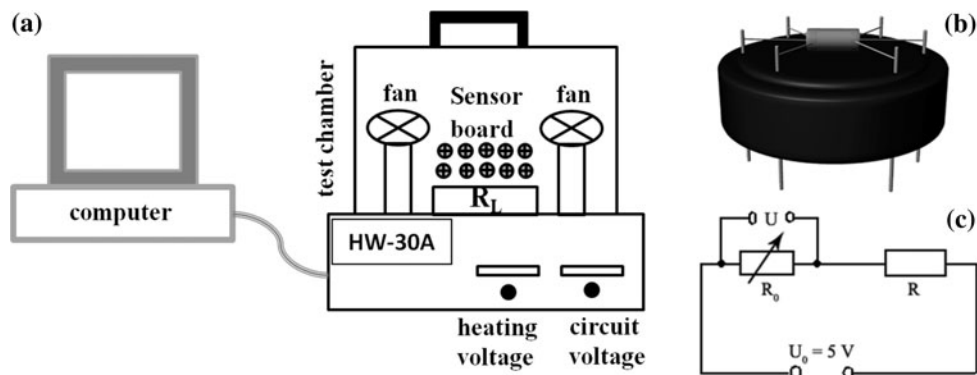
Measurement of gas-sensing

As-prepared samples were dispersed into an appropriate amount of ethanol under ultrasonication. Then, the formed suspension was coated onto the surface of the alumina ceramic tube and dried in air. Commercial ZnO powder based sensor has also been used for comparison. There are two Pt wires on each end of alumina tube, and a Ni–Cr alloy coil going through the tube employed as a heating filament to control the operating temperature by tuning the heating voltage. The gas-sensing measurements were taken on a commercial HW-30A system (Han Wei Electronics Co., Ltd., China) at a relative humidity of 25–33 %. HW-30A is a static system using atmospheric air as the interference gas. Test gases with calculated amount are introduced into the test chamber by a microsyringe. Two electric fans installed in the chamber are used to make test gas homogeneous. After test, the chamber was removed for test gases to diffuse away. The schematic and working principle are shown in Fig. 1. The gas response is defined as $S = R_a/R_g$, where R_a and R_g are the resistance of the sensor in air and in the target gas, respectively. The time taken by the sensor to achieve 90 % of the total resistance change is defined as the response time in the case of adsorption or the recovery time in the case of desorption.

Results and discussion

The XRD patterns of the samples before and after calcination are shown in Fig. 2a, b, respectively. The diffraction peaks of unannealed products (Fig. 2a) can be well-indexed

Fig. 1 a The schematic of HW-30A gas-sensing test system, b the schematic image of ZnO sensor, c the equivalent circuit of the gas-sensing test system



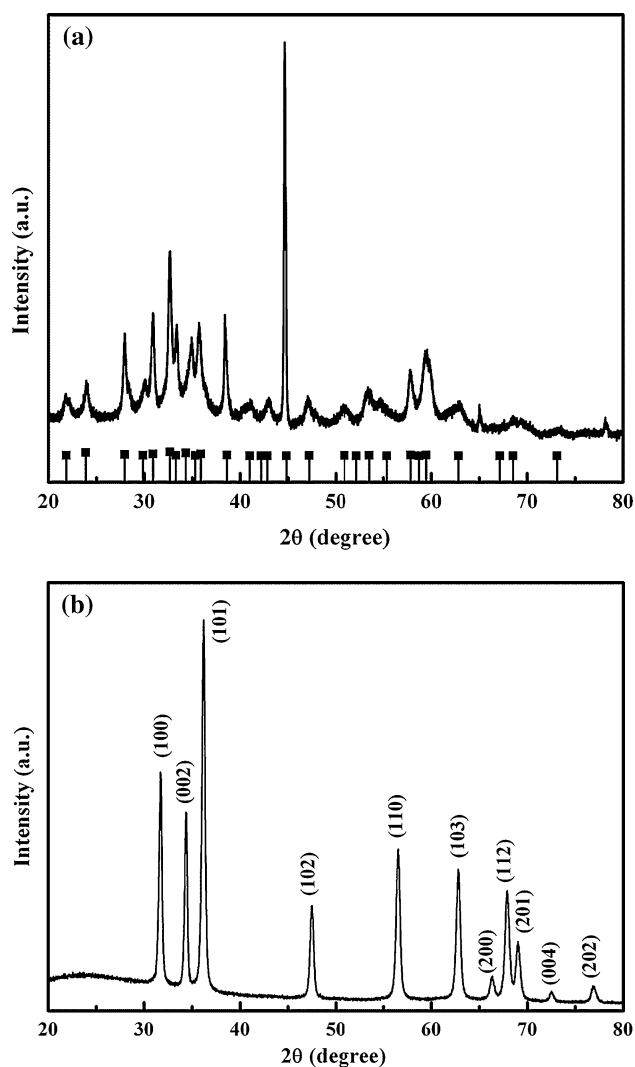


Fig. 2 The XRD patterns of the samples before (a) and after (b) calcinations. The standard diffraction of $\text{Zn}_4\text{CO}_3(\text{OH})_6\cdot\text{H}_2\text{O}$ is shown in the bottom of a as a reference

according to the Joint Committee On Powder Diffraction Standards (JCPDS) card (No. 11-0287), which indicates that the products are $\text{Zn}_4\text{CO}_3(\text{OH})_6\cdot\text{H}_2\text{O}$. After being annealed at 450 °C for 2 h, it is found that the diffraction peaks in each pattern match well with the hexagonal wurtzite ZnO reported in JCPDS card (No. 36-1451). No peaks due to impurities are detected, which reveals that all zinc salt precursors have been thoroughly decomposed into pure ZnO during anneal. The TGA-DSC curves were shown in Fig. 3. On the Wt curve, the first weight loss of 4 % between 25 and 140 °C corresponds to the removal of the water weakly adsorbed onto the surface of the nanoflakes. The second weight loss step of 26 % occurring between 140 and 290 °C (predominantly endothermic DSC peak at 260 °C) is ascribed to the release of water and carbon dioxide from the thermal decomposition of the precursor, which is consistent with the theoretical value.

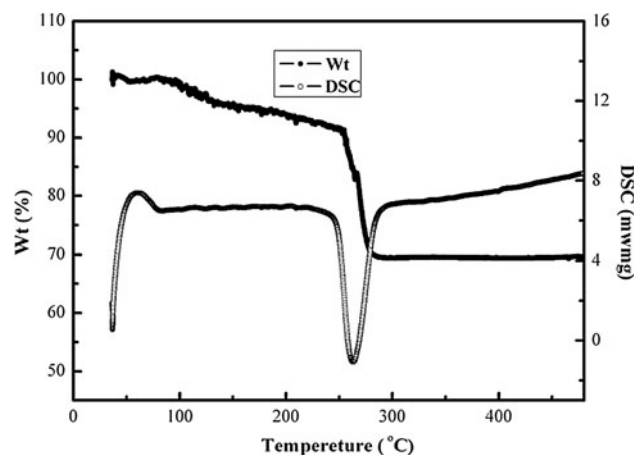


Fig. 3 The TGA-DSC curves of the precursor

The typical morphologies of the as-synthesized precursor and the porous products are shown in Fig. 4. It is clearly seen that the precursor was a sphere-like morphology (Fig. 4a), which is composed of numerous thin flakes. After the thermal treatment of the precursor at 450 °C for 2 h, the sphere-like morphology is maintained (Fig. 4b). Figure 4c, d are the side and front view of the flakes structures. It can be seen that the thickness of the flakes are about tens of nanometers and numerous, ultra-high dense pores with the size in tens of nanometers are formed through each flake. As seen in the TEM image (Fig. 4e), the porous structure is confirmed. Figure 4f, g are the HRTEM image from a ZnO crystalline grain and the corresponding selected-area electron diffraction patterns (SAED). The measured lattice spacing of 0.28 nm is consistent with the d-spacing of (100) lattice planes of the wurtzite-type ZnO, in agreement with the XRD results. Figure 5 displays the adsorption–desorption isotherm and BJH pore size distribution as the inset. The specific surface area was determined by multipoint BET method using the adsorption data in the relative pressure (P/P_0) range of 0.05–0.3. The ZnO spheres have a specific surface area of 38.4 m^2/g , which is higher than that of the commercial ZnO powder (7.1 m^2/g). According to the BJH pore size distribution curve (inset of Fig. 5), ZnO spheres exhibit a mesoporous structure with pore diameter centered at 8.67 nm.

It is well-known that the sensitivity of a semiconductor gas sensor is highly influenced by its operating temperature. In order to find the optimum operating condition of sensors, the sensors are exposed to 100 ppm $\text{C}_2\text{H}_5\text{OH}$ at different operating temperatures (Fig. 6). The response is found to increase with the operating temperature to a maximum (at 280 °C), about 25, and then decrease with further increment of the temperature. This decrement might be attributed to the competing desorption of the

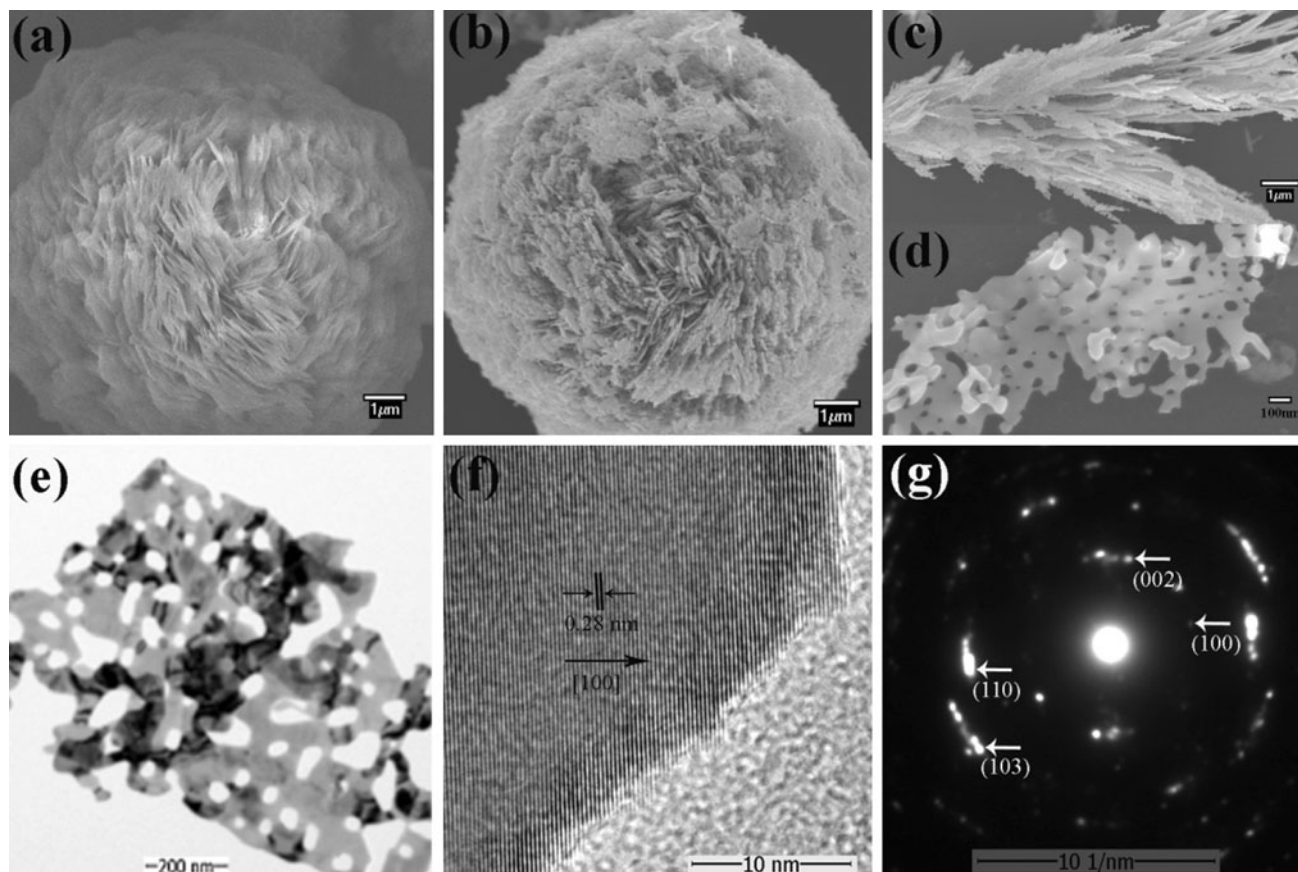


Fig. 4 SEM images of the hierarchical precursor $\text{Zn}_4\text{CO}_3(\text{OH})_6 \cdot \text{H}_2\text{O}$ (a) and ZnO (b), c slide view and d front view of porous ZnO flakes structure. e A TEM image of the single flake, g A typical HRTEM

image from a ZnO crystalline grain and f the corresponding diffraction patterns (SAED) from the ZnO flake

chemisorbed oxygen [17]. Therefore, 280 °C can be defined as the optimum operating temperature and applied in all the investigations hereinafter.

The transient response of the sensors based on ZnO spheres and commercial powder sensors at 280 °C to $\text{C}_2\text{H}_5\text{OH}$ with concentration varying from 2 to 500 ppm are demonstrated in Fig. 7. The response values of the two sensors increased rapidly as the ethanol gas is injected. In contrast, the response values return back to the initial state as the ethanol gas is released. It is obvious seen that the sensor based on the spheres exhibited enhanced responses for each concentration compared with that based on commercial powder. Although the exact fundamental mechanisms that cause a gas response are still controversial, it is responsible for a change of the carrier concentrations induced by chemical interaction of gas molecules with the surface of the sensing materials [18]. For the two gas sensors, the amount of active sites for oxygen and the reducing gases is important factor to their gas-sensing performance. The large specific surface area of the spheres composed of porous flakes provides more active sites, which leads to the enhanced performance.

Figure 8 illustrates the response of the sensor as a function of gas concentration. The response of the sensor increases with the gas concentration of $\text{C}_2\text{H}_5\text{OH}$. The sensor show obvious response to 2 ppm ethanol, with the corresponding response value of about 2.8. When exposed to 100 ppm ethanol, the response value has reached 25, which is comparable with the sensors based on ZnO nanostructures reported [19–22]. Hongsith et al. [19] reported ethanol sensors based on ZnO and Au-doped ZnO nanowires with the response lower than 10. Chen et al. [20, 21] reported the responses of the ZnO nanorod and nanotube sensors were about 8 and 24.1, respectively. However, it is smaller than the Pt-ZnO flower-based sensor [22]. The porous microstructure, which leads to the large effective surface area, may contribute a lot to the high response, due to the high porosity and large-specific surface area. The similar results have been reported widely [1, 14, 15].

Another interesting phenomenon is that there is a linear relationship between the response and the $\text{C}_2\text{H}_5\text{OH}$ concentration in the range of 2–500 ppm, as shown in Fig. 8, where the solid line is the linear fitting result. In fact the response of a semiconducting oxide is usually empirically

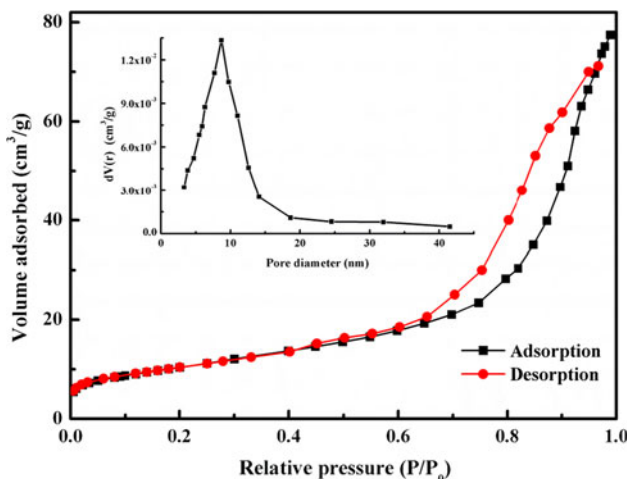


Fig. 5 The adsorption–desorption isotherm and BJH pore size distribution (the *inset*) curves of the obtained ZnO products

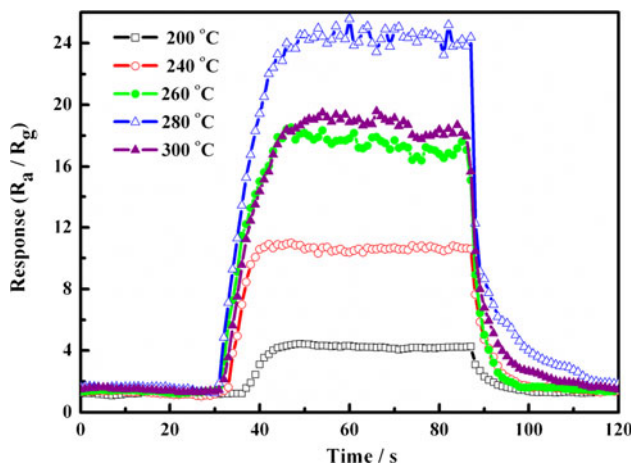


Fig. 6 The transient response of porous ZnO flakes sensor to 100 ppm C₂H₅OH at various operating temperatures

depicted as $S = A [C]^N + B$, where $[C]$ is the concentration of the target gas, and the sensitivity is characterized by the prefactor A and exponent N . N may have some rational fraction value (usually 1 or 1/2), depending on the charge of the surface species and the stoichiometry of the elementary reactions on the surface [23]. For porous ZnO flake sensor, N is 1. The sensor sensitivity to per ppm ethanol was 0.168, and the linear related coefficient (r) is 0.99. Such good linearity between the response and gas concentration provides potential application in quantitative measurement of C₂H₅OH concentration.

The response and recovery times are presented in Fig. 9. The gas sensor exhibits rapid gas-sensing behaviors when the ethanol gas is injected or released. It is seen that the response and recovery times were <30 and 20 s, respectively. This can be explained from the aspect of gas

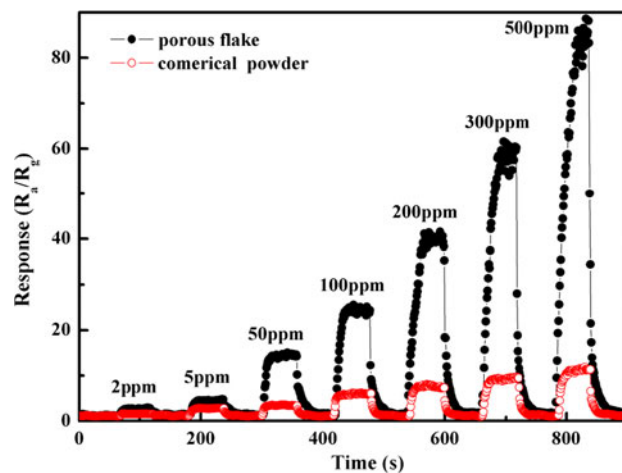


Fig. 7 The transient responses of sensors based on porous ZnO flakes and commercial ZnO powders to various concentrations of C₂H₅OH at 280 °C

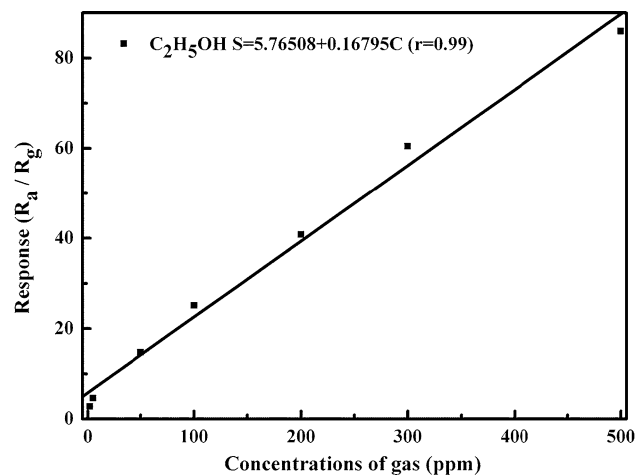


Fig. 8 The response of the sensor as a function of gas concentration. The *solid line* is the linear fitting results

diffusion. Assuming Knudsen flow, the diffusion coefficient of the target gas can be defined by the followed equation [24]:

$$D_K = \frac{\varepsilon d}{3\tau} \left(\frac{8RT}{\pi M} \right)^{1/2} \quad (1)$$

where D_K is the Knudsen diffusion coefficient in porous medium; ε , d , τ , R , T , and M are dimensionless porosity, pore diameter, dimensionless tortuosity, gas constant, temperature, and molar mass, respectively. From the equation presented above, the gas diffusion is directly proportional to the porosity and pore diameter, while it is inversely proportional to the pore tortuosity. In the ZnO spheres, numerous pores with the size in tens of nanometers distributed through each flake. Therefore, the ultrahigh pore density may be dominant among the three parameters

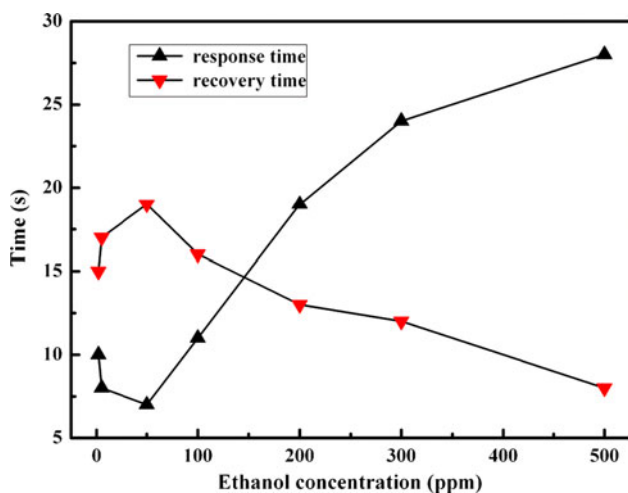


Fig. 9 The response and recovery times of ZnO sensor

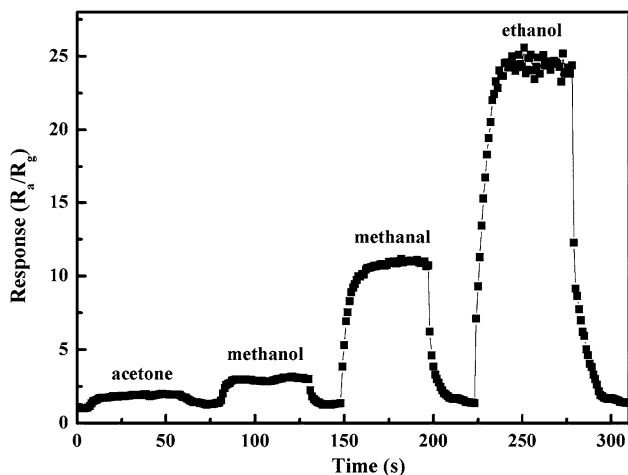


Fig. 10 The transient response of ZnO sensor to 100 ppm ethanol, methanol, methanal, and acetone at the operation temperature of 280 °C

presented above, and is suggested to allow fast adsorption and desorption.

Metal-oxide semiconductor nanomaterials have been usually used for the combustible and noxious gases detection. The cross sensitivity has been one of the significant issues. To examine the selectivity, the porous ZnO spheres sensors were exposed to other combustible gases, including methanol, methanal, and acetone. The measurements were operated at the temperature of 280 °C to the four kinds of gases with the concentration of 100 ppm, respectively. As can be seen in Fig. 10, the sensor is more sensitive to ethanol with the response value of 25, while only 3, 11, and 2 to methanol, methanal, and acetone, respectively, indicating that the sensor has selectivity to the ethanol gas.

The long-time stability is one of the most important characteristics for sensors. Figure 11 show the sensor

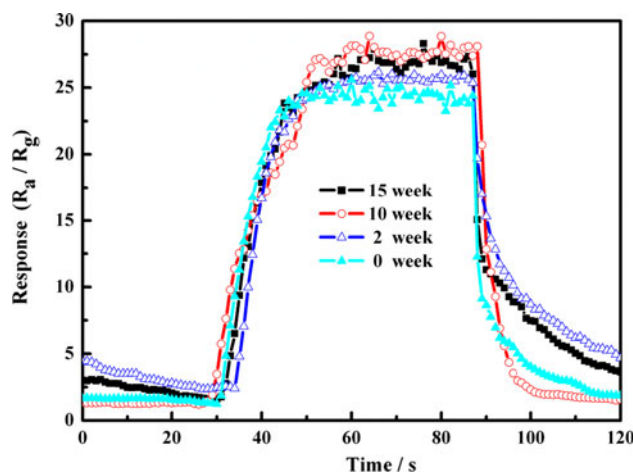


Fig. 11 The response of ZnO sensor to 100 ppm of C₂H₅OH at 280 °C after storage for various time periods

response versus the storing time. After first measurement, the sensor was stored in dry air for the sequent test. A series of tests were carried out at the times of 0, 2, 10, 15 weeks, with a 100 ppm ethanol concentration at the operation temperature of 280 °C. It was found that the variations of the sensor response are quite slight, without consideration of the instrument errors, indicating that the sensor device of ZnO sphere has long-term stability.

Conclusions

In summary, gas-sensor-based on ZnO spheres composed of the flakes with high-density pores sized in tens nanometers was fabricated. The porous ZnO spheres sensor has highest response, up to 25, to C₂H₅OH at 280 °C among C₂H₅OH, methanol, methanal, and acetone, and is reproducible after 15 weeks without considering the slight change in indoor environment and instrument errors. The concentration dependence of the sensor response was linear in the C₂H₅OH concentration range of 2–500 ppm at 280 °C. Result demonstrated that it is a facile way to prepare porous structure ZnO with superior ethanol gas-sensing performance.

Acknowledgements This study was supported by the National Natural Science Foundation of China (Grant No. 50602040, 11104253 and 10574112), and the Science and Technology Project on Key Problems of Henan Province (Grant No. 082101510007).

References

- Liu J, Guo Z, Meng F, Luo T, Li M, Liu J (2009) *Nanotechnology* 20:125501
- Stewart ME, Anderton CR, Thompson LB, Maria J, Gray SK, Rogers JA, Nuzzo RG (2008) *Chem Rev* 108:494

3. Venkatesan BM, Dorvel B, Yemenicioglu S, Watkins N, Petrov I, Bashir R (2009) *Adv Mater* 21:2771
4. Ahn MW, Park KS, Heo JH, Park JG, Kim DW, Choi KJ, Lee JH, Hong SH (2008) *Appl Phys Lett* 93:263103
5. Kauffman DR, Star A (2008) *Angew Chem Int Ed* 47:6550
6. Lee JH (2009) *Sens Actuators, B* 140:319
7. Seiyama T, Kato A, Fulishi K, Nagatani M (1962) *Anal Chem* 34:1502
8. Deng L, Ding X, Zeng D, Zhang S, Xie C (2012) *IEEE Sens J* 12:2209
9. Xu J, Chen Y, Li Y, Shen J (2005) *J Mater Sci* 40:2919
10. He L, Jia Y, Meng F, Li M, Liu J (2009) *J Mater Sci* 44:4326
11. Vanheusden K, Warren WL, Seager CH, Tallant DR, Voigt JA, Gnade BE (1996) *J Appl Phys* 79:7983
12. Korsunskaya NO, Borkocska LV, Bulakh BM, Khomenkova LY, Kushnirenko VI, Markevich IV (2003) *J Lumin* 102–103:733
13. Janotti A, Van de Walle CG (2005) *Appl Phys Lett* 87:122102
14. Hyodo T, Sasahara K, Shimizu Y, Egashira M (2005) *Sens Actuators, B* 106:580
15. Zhang J, Wang S, Wang Y, Wang Y, Zhu B, Xia H, Guo X, Zhang S, Huang W, Wu S (2009) *Sens Actuators, B* 135:610
16. Hosono E, Fujihara S, Honma I, Zhou H (2005) *Adv Mater* 17:2091
17. Bie LJ, Yan XN, Yin J, Duan YQ, Yuan ZH (2007) *Sens Actuators, B* 126:604
18. Barsan N, Weimar U (2001) *J Electroceram* 7:143
19. Hongsith N, Viriyaworasakul C, Mangkornong P, Mangkornong N, Choopun S (2008) *Ceram Int* 34:823
20. Chen J, Li J, Li JH, Xiao GQ, Yang XF (2011) *J Alloys Compd* 509:740
21. Chen YJ, Zhu CL, Xiao G (2008) *Sens Actuators, B* 129:639
22. Xue X, Chen Z, Xing L, Ma C, Chen Y, Wang T (2010) *J Phys Chem C* 114:18607
23. Wan Q, Li QH, Chen YJ, Wang TH, He XL, Li JP, Li CL (2004) *Appl Phys Lett* 84:3654
24. Veldsink JW, Van Damme RMJ, Versteeg GF, Van Swaaij WPM (1995) *Chem Eng J Biochem Eng J* 57:115